

TEMPERATURE STRUCTURE OF FOUR MERGING CLUSTERS OBTAINED WITH *CHANDRA*

M. MARKEVITCH, A. VIKHLININ, P. MAZZOTTA, L. VAN SPEYBROECK (SAO)

*Poster presented at X-ray Astronomy 2000, Palermo, September 4-8, 2000*

## ABSTRACT

We present preliminary *Chandra* results on  $z \approx 0.2$  clusters A665, A2163 and A2218, and a  $z = 0.05$  cluster A754. For A754, A665 and A2163, we have derived first high-resolution projected gas temperature maps. All three show strong spatial temperature variations in the inner  $r < 0.5 - 1 h_{50}^{-1}$  Mpc regions, indicating ongoing mergers. The maps reveal a probable shock in front of a moving cluster core in A665, a rather complicated temperature distribution in the center of A2163, and possibly a merger of three subclusters in A754. At greater off-center distances, radial profiles for A2163 and A2218 show a temperature decline, in agreement with earlier *ASCA* results.

## INTRODUCTION

Clusters of galaxies, the biggest collapsed mass aggregations in the present universe, are formed through the hierarchical process of gravitational infall, collision and merging of smaller groups and clusters and a subsequent relaxation of all the matter components in the cluster. Each merger is a very energetic event. A large fraction of the kinetic energy of the collision goes into shock heating of the intracluster gas (e.g., Schindler & Müller 1993; Roettiger et al. 1993 and later works), a process that has great importance for cluster physics and that we can readily observe using the *Chandra*'s combination of energy coverage and superb spatial resolution. Here we present preliminary results from ACIS-I on four hot clusters, A665, A2163, A2218, and A754. X-ray images of all these clusters show structure of various degrees of complexity; however, in the absence of the characteristic temperature signatures, it may be a result of projection rather than a merger. For A754, unambiguous data existed before that it is a merger, from both the optical and X-ray temperature data (Zabludoff & Zaritsky 1995; Henry & Briel 1995; Henriksen & Markevitch 1996). For A2163, some indication of a nonrelaxed state from the gas temperature and optical data existed (Markevitch et al. 1994; Squires et al. 1997); and for A2218, weak lensing mass reconstruction suggested two mass concentrations (Kneib et al. 1996). For A665, there has been no suggestion of a nonrelaxed state other than an asymmetric X-ray image. A665, A2218 and A2163 also are famous SZ sources (e.g., Birkingshaw et al. 1991, references therein and later works) and detailed gas temperature maps are critical for correct interpretation of the SZ data.

## DATA ANALYSIS

A665, A2163 and A2218 were observed by ACIS-I for short exposures of 9 ks, 10 ks, and 18 ks, respectively (clean exposure after the rejection of background flares, if

any), which is sufficient for derivation of crude temperature maps and radial temperature profiles. A754 was observed by ACIS-I for a clean exposure of 39 ks, sufficient for a detailed temperature map of the central  $16' \times 16'$  region covered by ACIS-I.

The ACIS gain tables, quantum efficiency curves and spectral response matrices latest as of September-October 2000 were used. The detector + sky background was estimated using the appropriate blank sky datasets, correcting for a slow secular decrease of the background rate (Markevitch 2000). The background uncertainty of  $\pm 5\%$  was included in quadrature to the statistical uncertainties of the temperature values (it is significant for the radial profiles at high radii). Point sources were excluded from the analysis, and the energy band of 0.8–9 keV (or close) was used. The CTI-induced nonuniformity of the ACIS-I quantum efficiency was corrected using an approximate model function (Vikhlinin 2000). For the A754, A665 and A2218 observations made at the  $-110^{\circ}\text{C}$  ACIS temperature, this correction is important, while for A2163 observed later at  $-120^{\circ}\text{C}$ , it is much less significant. We also used an additional experimental position-independent correction factor of  $\approx 0.9$  for the ACIS-I quantum efficiency below  $E = 2$  keV to account for the difference between ACIS-S3 and ACIS-I observations of a calibration SNR (Vikhlinin 2000). For hot clusters, ignoring it results in spuriously high Galactic absorption columns and temperatures and their dependence on the adopted lower energy cut. Once these corrections were applied, all fits were acceptable and independent of the energy band used. The absorption column was fixed at the Galactic values for A754, A665 and A2218, and at the *ROSAT* PSPC value for A2163 (which is higher than the Galactic one, Elbaz et al. 1994); fitting it as a free parameter gave consistent values. Temperatures for the radial profiles were fit using XSPEC, and two-dimensional temperature maps were derived from adaptively smoothed ACIS images in a number

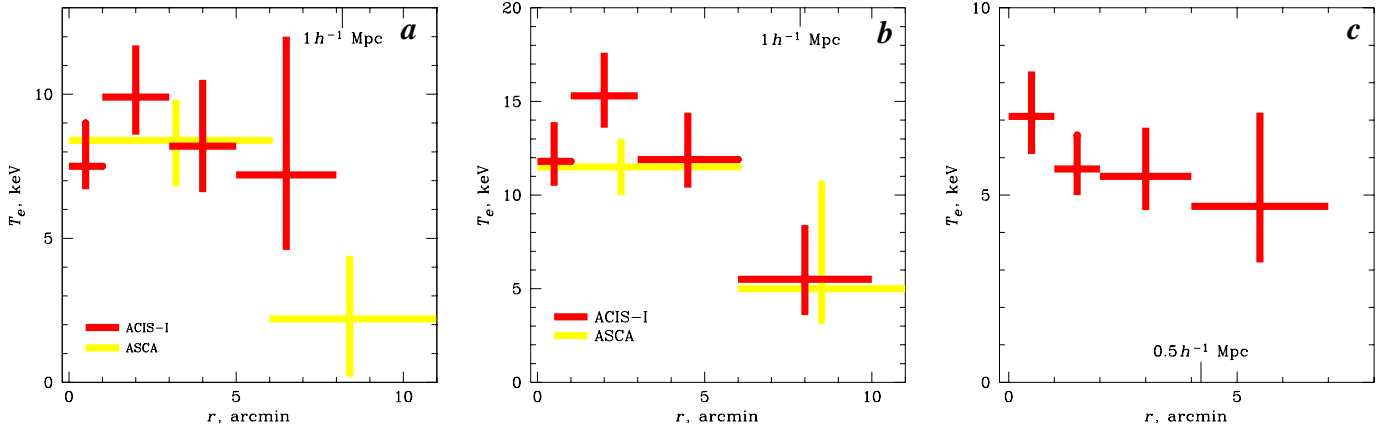


FIG. 1.—Projected radial temperature profiles of (a) A665, (b) A2163, (c) A2218. The A665 and A2163 profiles are overlaid on the ASCA results from Markevitch (1996).

of narrow energy bands as described in Markevitch et al. (2000).

#### RESULTS AND DISCUSSION

Figure 1 presents radial temperature profiles for the three distant clusters, overlaid on the ASCA projected profiles for A665 and A2163 from Markevitch (1996). The profiles for A2163 and A2218 show a radial decline — for A2163, in good agreement with the ASCA result from Markevitch (1996), and for A2218, with that from White (2000). The A665 profile is consistent with a constant temperature, although it does not cover the complete radial range of the ASCA data.

However, the A665 temperature map (Fig. 2) shows that this cluster is in fact highly nonisothermal — there is a spectacular bow shock in front of what appears from the image to be a cooler cluster core moving from the NW direction with respect to the gas in the Southern region.

Figure 3 shows a temperature map of A2163. Already the brightness contours of the ACIS image show that the cluster inner region is probably in a highly nonrelaxed state. The temperature map confirms that and reveals hot gas regions coincident with enhancements in the gas density that most plausibly are shocks or streams of shock-heated gas. The central region is cooler in projection, perhaps because the shocks have not penetrated the dense subcluster cores as they fell to the center, similarly to

what we see in A2142 and A3667 (Markevitch et al. 2000; Vikhlinin et al. 2000). Temperature maps for A2163 and A665 and their relation to the radio data will be discussed in detail in the forthcoming paper.

Figure 4 shows a detailed temperature map for A754. On a large scale, it is in good agreement with earlier results from Henry & Briel (1995) and Henriksen & Markevitch (1996). The latter’s ASCA map had only  $3 \times 3$  pixels in the area shown in Fig. 4. Large hot area South and Southwest of center and smaller hot regions elsewhere most plausibly result from shock heating. There is a curious low-temperature region at the tip of the elongated dense gas body; it does not coincide with either the gas density peak or one of the two cD galaxies in this cluster. A close examination of the optical image reveals a possible small galaxy group at this position, and a simple estimate shows that the elongated body may in fact be a projection of two more round subclusters of different temperatures, making A754 a three-body merger. A more detailed discussion will be presented in a forthcoming paper.

The results presented here are made possible by the successful effort of the entire *Chandra* team to launch and operate the observatory. We thank Bill Forman, Christine Jones, Dan Harris, Larry David, Paul Nulsen, Hank Donnelly, Dong-Woo Kim and others for useful discussions.

#### REFERENCES

Birkinshaw, M., Hughes, J., & Arnaud, K. 1991, ApJ, 379, 466  
 Elbaz, D., Arnaud, M., & Böhringer, H. 1995, A&A, 293, 337  
 Henriksen, M., & Markevitch, M. 1996, ApJ, 466, L79  
 Henry, J., & Briel, U. 1995, ApJ, 443, L9  
 Kneib, J. P., Ellis, R. S., Smail, I., Couch, W. J., Sharples, R. M. 1996, ApJ, 471, 643  
 Markevitch, M. 1996, ApJ, 465, L1  
 Markevitch, M. 2000, *Chandra* calibration memo  
 (<http://asc.harvard.edu/cal/>, sections “ACIS”, “Background”)  
 Markevitch, M., et al. 2000, ApJ, 541, 542  
 Markevitch, M., Yamashita, K., Furuzawa, A., & Tawara, Y. 1994, ApJ, 436, L71  
 Roettiger, K., Burns, J., & Loken, C. 1993, ApJ, 407, L53  
 Schindler, S., & Müller, E. 1993, A&A, 272, 137  
 Squires, G., Neumann, D., Kaiser, N., Arnaud, M., Babul, A., Böhringer, H., Fahlman, G., Woods, D. 1997, ApJ, 482, 648  
 Vikhlinin, A. 2000, *Chandra* calibration memo  
 Vikhlinin, A., Markevitch, M., & Murray, S. 2000, ApJ, submitted (astro-ph/0008496)  
 White, D. 2000, MNRAS, 312, 663  
 Zabludoff, A., & Zaritsky, D. 1995, ApJ, 447, L21

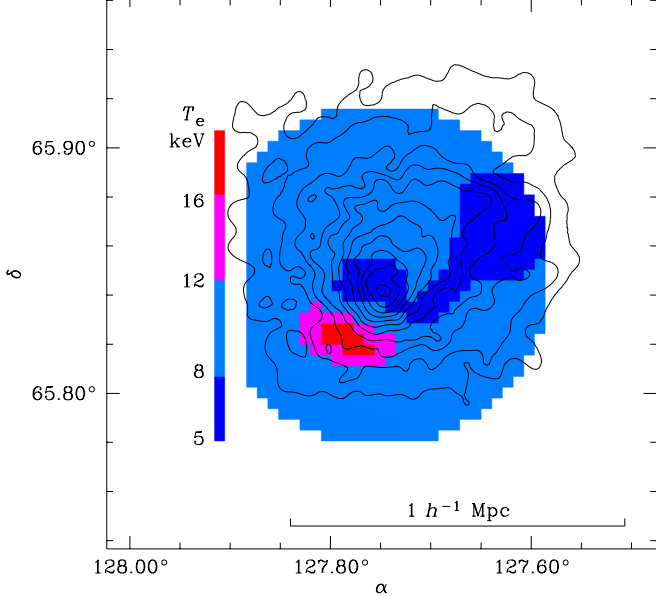


FIG. 2.—Temperature map of A665. Contours show ACIS-I 0.5–4 keV image (point sources removed), while colors show projected gas temperature. There is a hot region “in front” of the cluster core and a distinct trace of cooler gas from North-West towards the center, generally following the gas density elongation.

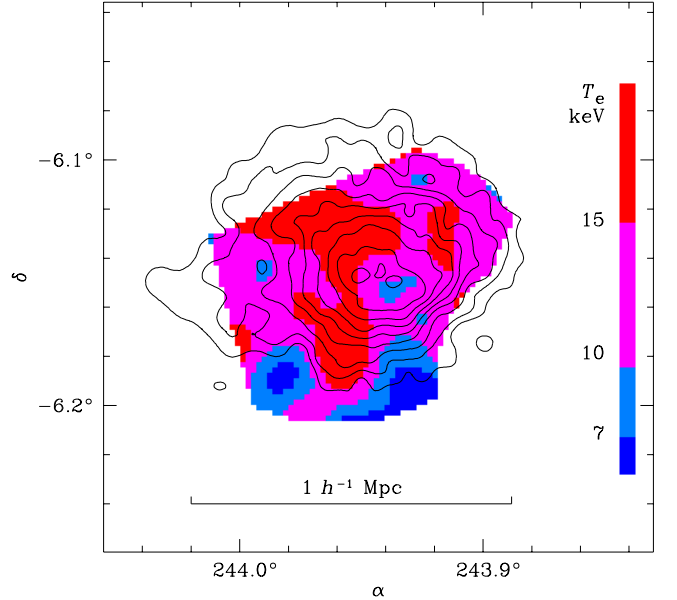


FIG. 3.—Temperature map of A2163. Contours show ACIS-I 0.8–4.5 keV image (point sources removed), while colors show gas temperature (areas with high statistical errors are removed). The image shows a lot of structure, and the temperature structure generally follows that in the gas density.

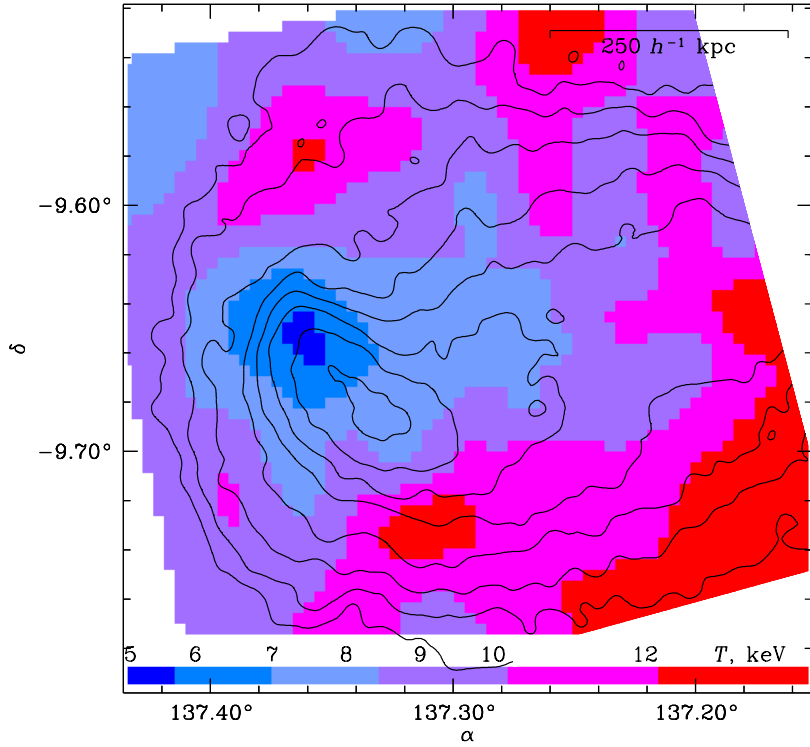


FIG. 4.—Temperature map of A754. Contours show ACIS-I 0.8–6 keV image (point sources removed), while colors show gas temperature. The cold spot does not coincide with either the gas density peak or one of the cD galaxies.